

## Full Paper

# Quantitative Estimation of Residual Stresses in Quenched Steel through Ultrasonic Parameters

Supun Rangana\*, Gihan Ishara, Sivahar Vigneswaran, and Gayan Aravinda

Department of Materials Science and Engineering, Faculty of Engineering, University of Moratuwa, Sri Lanka

Corresponding Author: [srangana78@gmail.com](mailto:srangana78@gmail.com)

Received: 04 July 2023; Revised: 15 August 2024; Accepted: 21 August 2024; Published: 19 January 2025

### Abstract

Generally, residual stresses are present in the metal specimens after manufacturing and heat treatment processes. Quenching is a heat treatment process that forms residual stress in metals. Two testing methods are used to find residual stresses in the industry, which are Destructive and Non-Destructive. This research is focused on estimating residual stresses in quenched AISI 1045 Medium carbon steel using the Ultrasonic testing method as a non-destructive method. Water, Saltwater, and oil were used as three different quenching media to perform the quenching process. Ultrasound attenuation was used to measure the residual stresses in quenched steel, considering the difference in the attenuation coefficient before and after quenching. 12 mm thick AISI 1045 type steel sample was used to give the tensile stress, and the ultrasonic attenuation coefficient difference in stressed and zero-stressed conditions was measured. The obtained data were used to correlate the variation of stresses with the attenuation coefficient difference. Using this correlation and attenuation coefficient difference before and after quenching, we can estimate the residual stress of quenched steel samples. ABAQUS modeling software was used to simulate residual stresses. The Von Mises stress criterion was considered to be the simulation residual stress result. Those experimental and simulation values were compared for an identical correlation for residual stresses. The specimen's Centre Plane Von Mises stress criteria were considered to obtain the simulation stress values for comparison as maximum residual stresses occur in the Centre plane of the specimen. According to the experimental and simulation residual stress values, there is a Similarity between those values. Therefore, this methodology can be used to measure the internal residual stresses in quenched steel samples.

**Keywords:** attenuation, quenching, residual stress, ultrasound, von mises criteria

---

### Introduction

The remaining stresses inside the material after manufacturing or heat treatment, without any external loads or thermal gradients, are called Residual stresses [1]. The residual stresses occur in engineering materials for several reasons, such as heat treatment and welding processes (phase transformations) and fabrication processes like forging, rolling, drawing, and extrusion [2]. Residual stress can significantly affect the engineering properties of materials (such as plasticity, toughness, elasticity, ductility, strength, etc.), distortion, fatigue life, dimensional accuracy, corrosion resistance, and brittle fracture. These effects usually lead to considerable expense in repairing and restoring parts, equipment, and structures. Moreover, such effects can lead to massive destruction. Accordingly, for these reasons, residual stress analysis is a critical stage in designing the part and structural components and estimating their reliability under actual service

conditions. Quenching is the heat treatment process used to obtain specific material properties of carbon steel. In the quenching process, the object is rapidly cooled from the Austenitizing temperature to room temperature to obtain certain material properties. The mainly employed quenching methods involve immersion, splash, or film cooling. Immersion cooling for which a workpiece is submerged in an unmoved or agitated liquid. Three test pieces were subjected to immersion cooling using water, oil, and salt water as the quenching mediums. Residual stresses are formed due to this rapid cooling. Also, many factors, such as quenchant type, quench severity, quenching process variables, the geometry of the component, and material properties, significantly affect the evolution of residual stresses. The heat transfer from the metal surface to the quench medium is the critical physical phenomenon that drives the microstructure evolution and residual stresses during quenching. The non-uniformity in heat transfer between the heated metal and the quench medium is the key source of residual stress development in the quenched material [3, 4]. Residual stress measurement is a significant and useful factor in manufacturing. There are two methods used in the industry: destructive and non-destructive. The most common destructive techniques are hole drilling, ring core, and bending deflection. The most common non-destructive techniques are the X-ray diffraction technique, Neutron technique and Ultrasonic technique. Ultrasound attenuation was used to find residual stresses in quenched steel in this research. Longitudinal waves and pulse echo techniques were used to identify the attenuation [5]. The ultrasonic method is an alternative, non-destructive, portable technique designed to assess residual stresses. ABAQUS standard modelling software was used to estimate the residual stress in quenched steel computationally, and Von Mises stress criteria were used to analyze those stresses [6, 7]. Considering Von Mises stress criteria, we can predict whether a given material will yield or fracture. Von Mises criteria are widely used for ductile materials, such as metals. The formula of Von Mises criteria is used to combine the three principal stresses into equivalent tensile stress. Experimental and simulation residual stress values were compared considering the Von Mises stress criteria of the center plane in the modeling test specimen.

## Materials and Methods

### Materials

AISI 1045 equivalent medium carbon steel was used as the material for the experiment, and Chemical compositions are given below.

**Table 1.** Chemical composition

Element	C	Si	Mn	P	S	Cr	Ni	Al	Nb	V	Fe
Percentage (%)	0.41	0.31	0.80	0.033	0.036	0.209	0.047	0.0155	0.074	0.0028	98

### Method

Attenuation occurs due to diffraction, absorption, and scattering by the interaction between the ultrasonic

waves and the grains [8]. Attenuation in steel-like materials is mainly caused by scattering at grain boundaries [9]. So, diffraction and absorption attenuation can be negligible in our study. The scattering from grain boundaries is also stress-dependent [10]. The value of this attenuation mainly depends on the grain size [9]. In the case of the quenching process, grain dimensions are changed. The residual stress will result in a change in these microscopic dimensions. When we consider the grain size effect on attenuation, it also depends on the wavelength ( $\lambda$ ) of the ultrasound beam. If the average grain size ( $d$ ) is less than one in twenty wavelengths, we can see a negligible grain size effect on attenuation [5, 11, 12]. Therefore, the effect due to grain dimensions changes during quenching can be negligible, because martensite microstructure is a very fine needle-shaped structure that is smaller than ferrite pearlite microstructure.

$$d \leq \frac{\lambda}{20}$$

For our study, we used a 5 MHz probe.

According to,  $V = f\lambda$  (Ultrasonic wave velocity in steel nearly  $5920 \text{ ms}^{-1}$ )

$$\text{Wavelength, } \lambda = \frac{5920}{5 \times 10^6}$$

$$\lambda = 1.184 \text{ mm}$$

$$\text{So, } \frac{\lambda}{20} = 0.0592 \text{ mm} = 59.2 \mu\text{m}$$

The microstructure image was obtained using an optical microscope to get the idea about grain size. AISI 1045 steel has ferrite and pearlite combined microstructure with nearly 50% ferrite and 50% pearlite. Pearlite has coarse grains than ferrite grains in the microstructure. The average grain size of this microstructure is less than  $50 \mu\text{m}$ . So, we can also negligible grain size effect on ferrite pearlite structure.

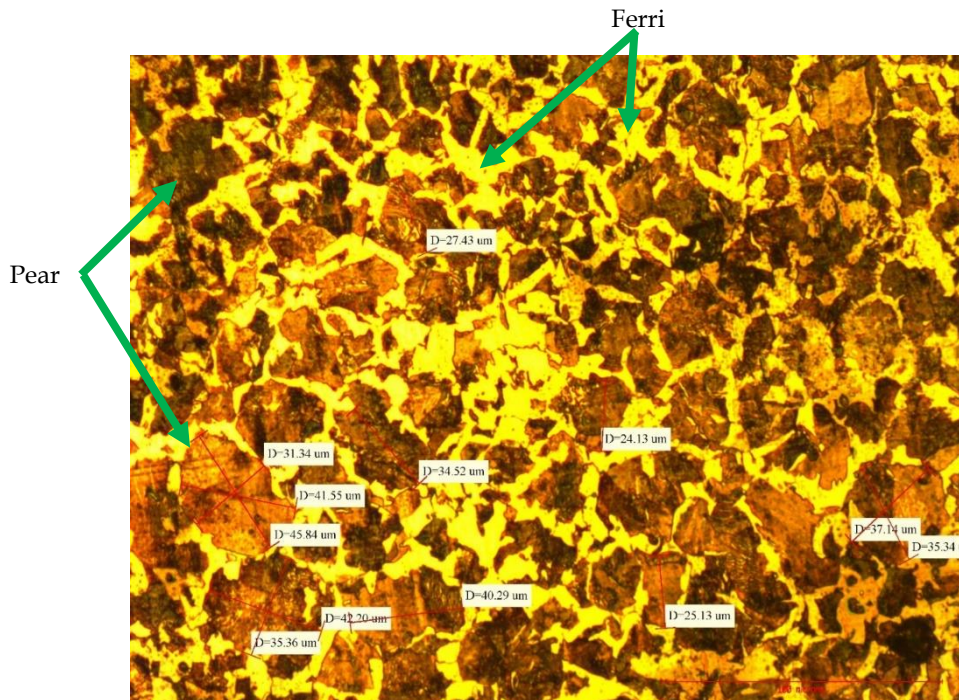


Figure 1. Microstructure with grain size

Ultrasonic attenuation was considered to find the residual stresses in this research. Olympus EPOCH 600 ultrasonic flaw detector with 5 MHz probe was used to obtain the attenuation coefficient. The attenuation coefficient was obtained considering the second and fourth back wall echoes. The below equation was used to find the attenuation coefficient  $\alpha$ ,

$$\alpha = (A_1 - A_2)/4d$$

Where  $\alpha$  is the attenuation coefficient, A1 and A2 are the second and fourth back wall echoes, and d is the thickness of the sample, respectively [13]. The ultrasonic attenuation coefficient was obtained before and after quenching from samples prepared for heat treatment. In the same dimension, three samples were quenched in three different quenching media: water, salt water, and oil. Three samples were heated from room temperature to 850 °C for 2 hours and kept for 1 hour at 850 °C.

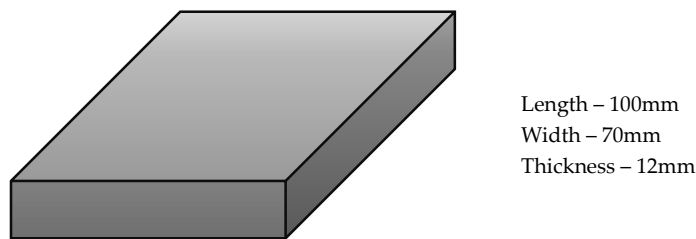


Figure 2. Sample dimensions

Considering those attenuation coefficients, attenuation coefficient differences were calculated for quenched samples. The attenuation data was obtained through the thickness and mutually perpendicular directions. Five data points were obtained for one direction. Those attenuation coefficient differences were plotted with distance. Also, one sample was used to give the load and measure the attenuation coefficient. A standard tensile test specimen of AISI 1045 type of 12 mm thickness was mounted in the universal testing machine, and the attenuation reading was obtained using the ultrasonic flaw detector. Tensile stress was changed step by step, starting from zero to 300 MPa. Ultrasonic attenuation measurements were obtained initially at zero load conditions and then during loading at uniform intervals of 25 MPa up to the maximum load of 300 MPa. Readings were acquired perpendicular to the stress direction.



Figure 3. Experimental setup

Then calculated the attenuation coefficient differences between the stress state and zero stress state and plotted that attenuation difference with relevant stress value. Considering those plotted graphs, we can find the value for residual stress that occurred due to quenching. A coupled temperature displacement was performed using ABAQUS finite element analysis to simulate quenching residual stresses. Due to symmetry, only half of the specimen was modeled because the highest stresses have occurred in the center plane of the test piece. Boundary conditions were set to allow convective heat transfer from the surface. Center plane was considered adiabatic and were restricted to move perpendicular to the planes to simulate the symmetry conditions. Film condition and coupled temperature-displacement settings were used to define the convection coefficient at the surface and to facilitate heat transfer and material flow simultaneously.

Two steps were defined for running the simulation. In the first step, the rectangular shape test piece was uniformly heated to the initial temperature. In the next step, quenching was performed. The sink temperature (or the quenchant temperature) was specified for performing the second step. The simulation was run for a period of the 1800s to reach equilibrium. This ensured that the quenching was continued till the test specimen reached sink temperature, uniformly throughout [6]. Different mesh sizes were done and get the optimum mesh size for results evaluation, and Von-Mises stress criteria were considered to result in analysis.

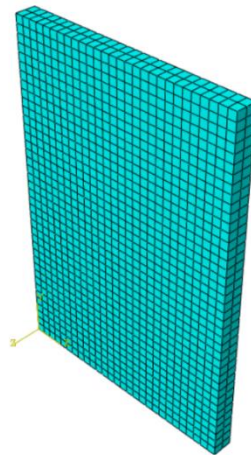


Figure 4. Mesh size

Density, Thermal conductivity, Specific heat capacity, Thermal expansion coefficient, Young's modulus, and Proof stress were used for modeling. Thermal expansion coefficient and density were assumed to be temperature-independent. Other properties were assumed to be temperature-dependent.

## Result and Discussion

Ultrasonic attenuation was measured using 2<sup>nd</sup> and 4<sup>th</sup> back wall echoes. Experimental results are presented in Figure 4, where the attenuation difference at 5 MHz is plotted versus applied stress, and 2<sup>nd</sup>-order polynomial relationships can be obtained for those data points with a good correlation coefficient of 0.9817.

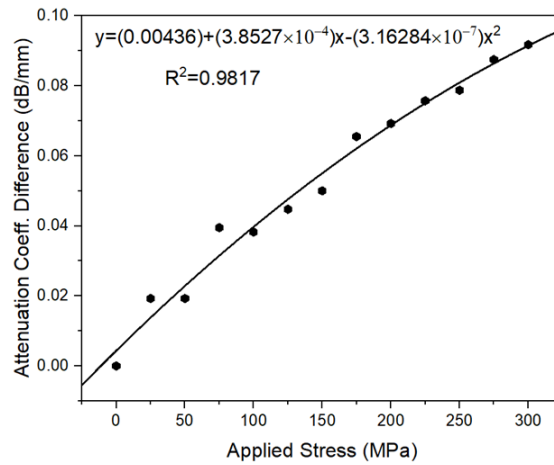


Figure 5. Attenuation coefficient difference with applied tensile stress

The attenuation difference gradually increases with the increase in applied stress because the scattering attenuation effect is enhanced with the increase in stress [8]. Then, we can obtain the residual stresses in quenched steel using the above stress-attenuation correlation and attenuation difference in quenched steel samples. Considering the attenuation caused by the residual stresses and applied stresses both occur mainly due to scattering attenuation; therefore, the correlation between applied stress and ultrasonic attenuation difference can fit with the residual stress and its ultrasonic attenuation difference [14].

The graphs illustrate the variations in the attenuation coefficient for saltwater, water, and oil quenching as a function of distance, offering a comprehensive analysis of how the attenuation coefficient changes with different quenching media.

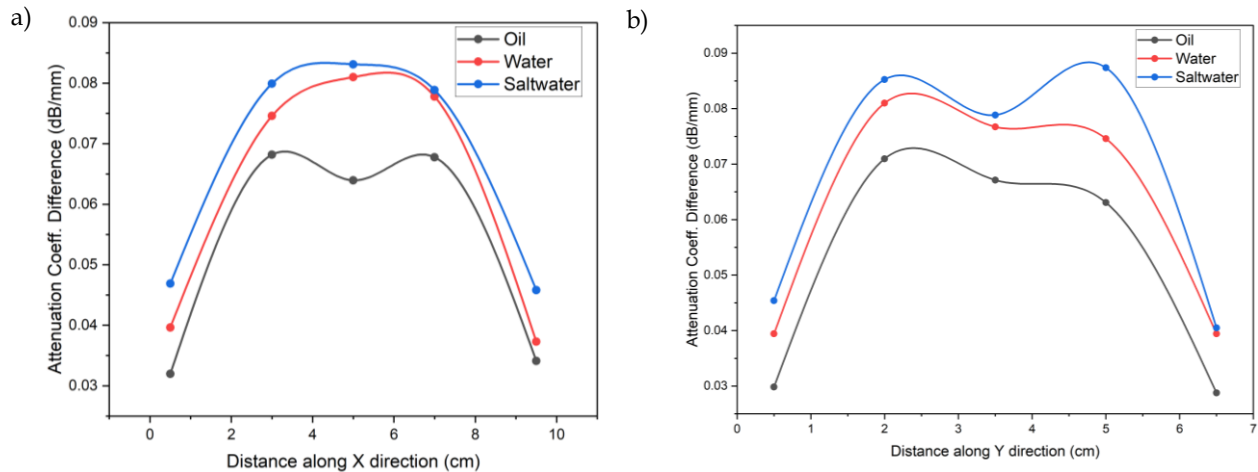


Figure 6. Attenuation coefficient difference with distance according to quenching medium (a) along x direction and (b) along y direction)

The graphs show the variations in the residual stress for saltwater, water, and oil quenching as a function of distance derived from the attenuation coefficient and the stress-attenuation correlation obtained from the Figure 5 graph.

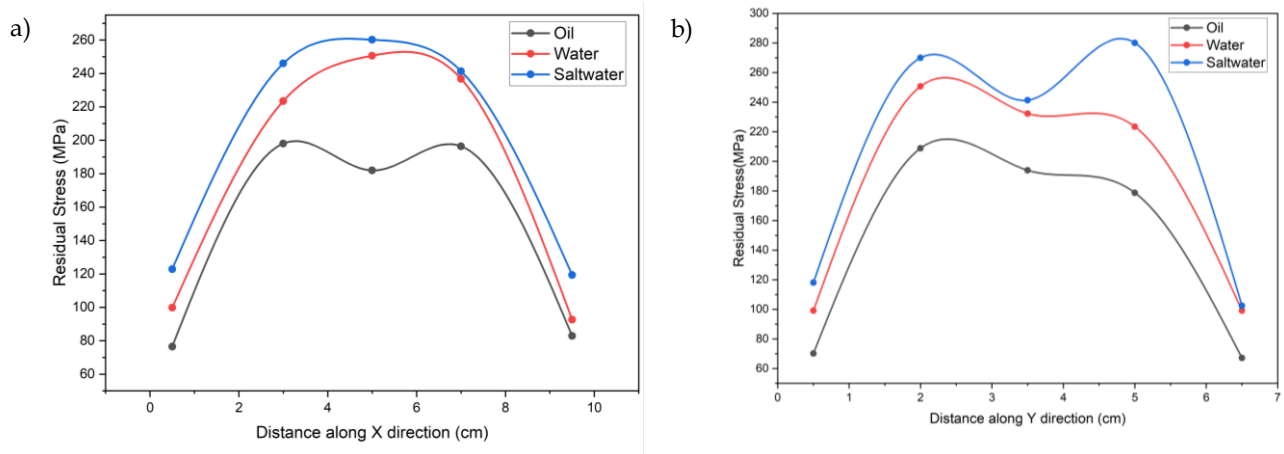


Figure 7. Residual stress magnitude with distance according to quenching medium (a) along x direction and (b) along y direction)

Von Mises stress criteria was considered to obtain the simulation residual stress values.

- For Saltwater Quenching.

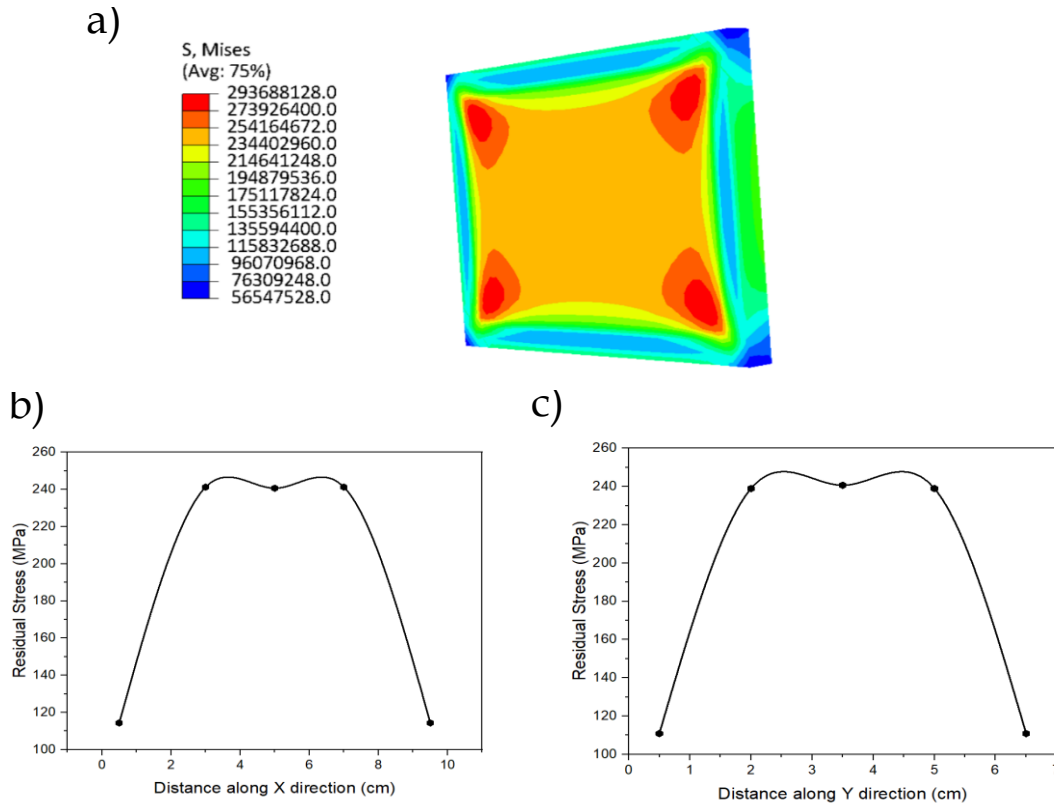
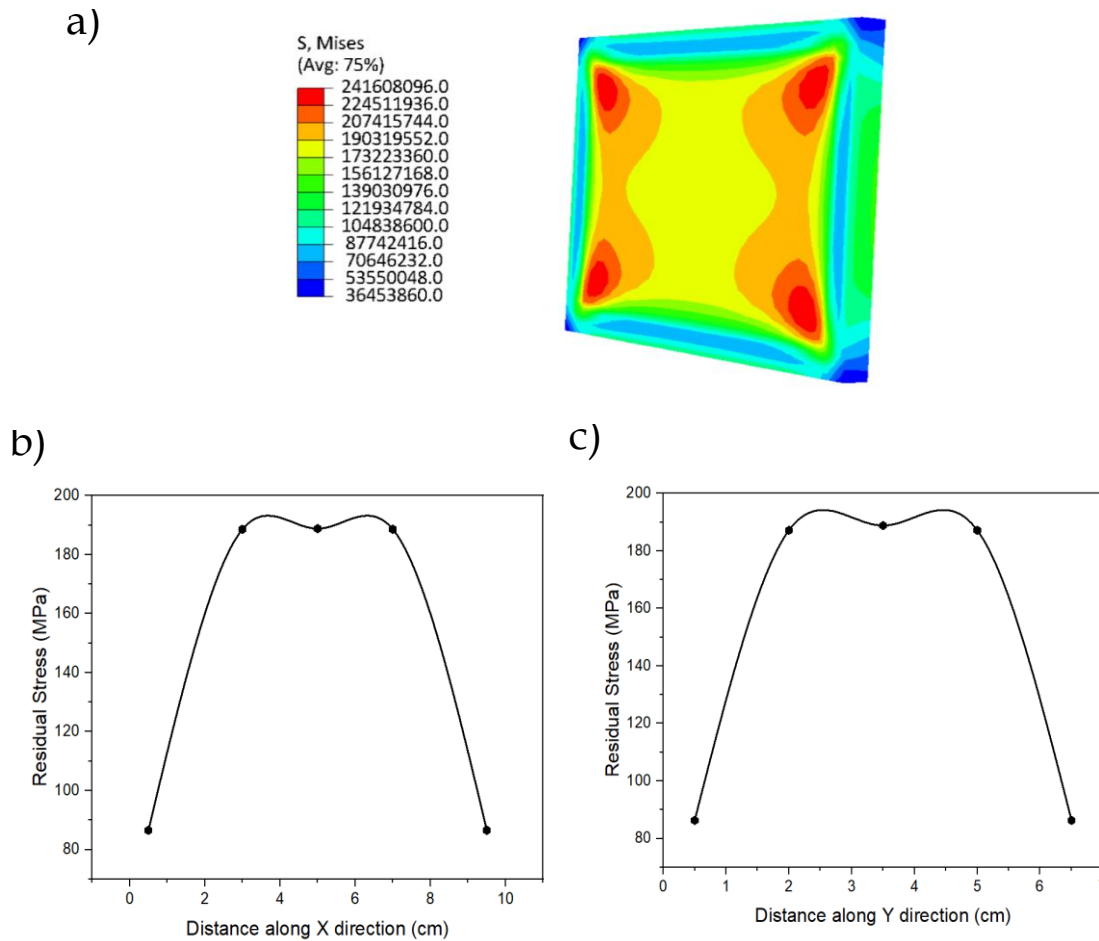


Figure 8. Simulation stress values for saltwater quenching (a) residual stresses of half model, (b) center plane residual stress along x direction, and (c) center plane residual stress along y direction)

- For Water Quenching.



**Figure 9:** Simulation stress values for water quenching (a) residual stresses of half model, (b) center plane residual stress along x direction, and (c) center plane residual stress along y direction)

Comparing the use of three different quenching media - saltwater, water, and oil - it becomes evident that the maximum residual stress occurs when quenching with saturated saltwater as evident of Figure 7. This is primarily attributed to saltwater significantly higher thermal conductivity compared to water and oil. When thermal conductivity is high, it enables rapid heat removal from the material. Consequently, the cooling rate during quenching becomes more severe, inducing higher thermal gradients within both the material's outer surface and interior [15]. This pronounced cooling rate disparity creates substantial temperature differences between the surface and the core of the material. As a result, differential thermal expansion and contraction occur, generating higher levels of internal stress. These conditions are particularly conducive to the development of maximum residual stresses.

- For Oil Quenching.

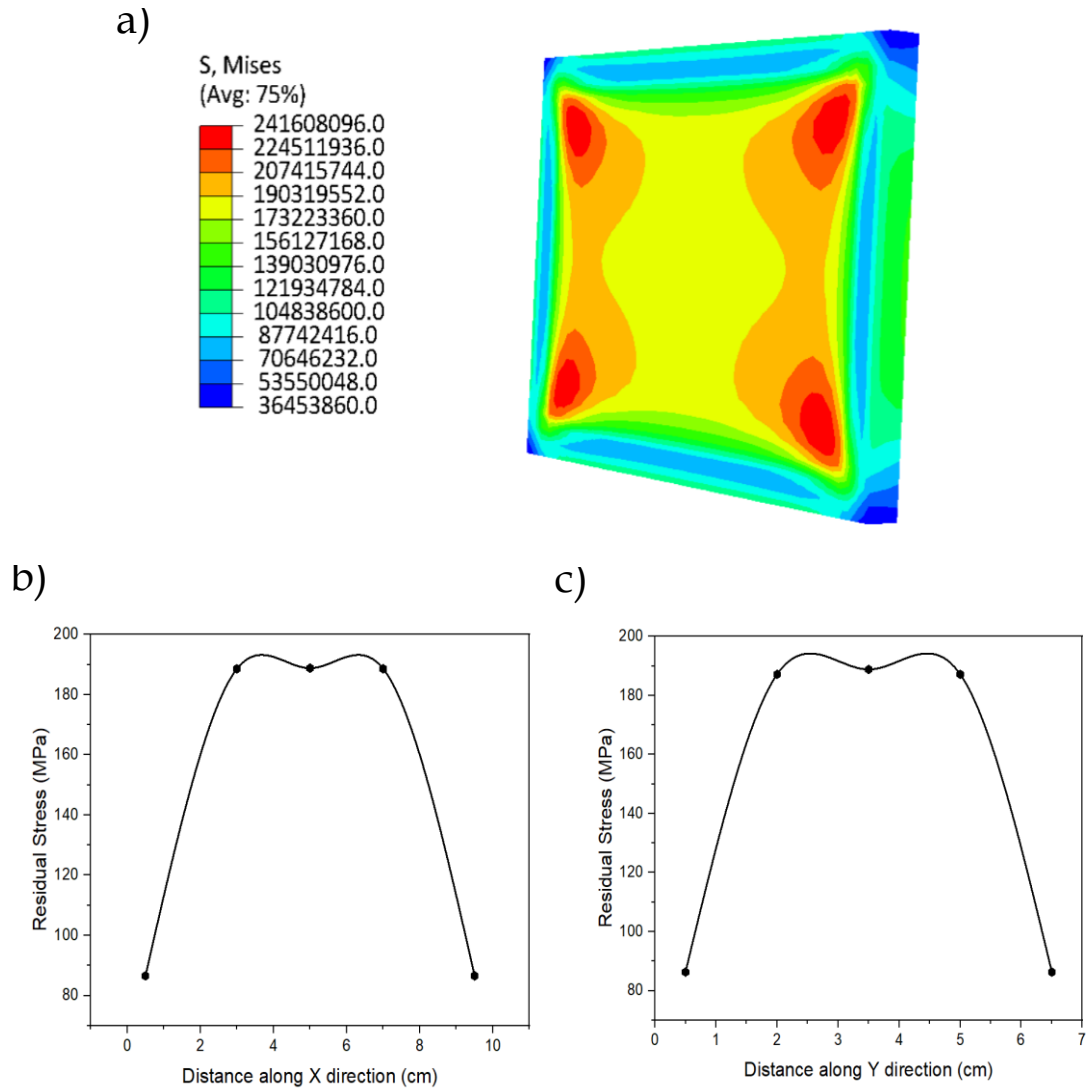


**Figure 10.** Simulation stress values for oil quenching (a) residual stresses of half model, (b) center plane residual stress along x direction, and (c) center plane residual stress along y direction)

Experimental and simulation residual stress values were compared to establish the correlation between those values. (Center plane Von Mises stress values were considered for this comparison. Because the center plane has maximum Von Mises stresses)

Figures 8, 9, and 10 show that simulation residual stress values are identical at points equidistant from the center of the rectangular test piece. This can be attributed to the geometric symmetry of the test piece and the uniformity of the quenching process in the simulation. The test piece's symmetric shape and uniform quenching ensure that equidistant points from the center experience similar thermal histories, resulting in consistent heat distribution and cooling rates along the centerline. This uniformity leads to symmetric thermal gradients and stress distributions, causing residual stresses to mirror each other across the

centerline. Consequently, points at the same distance from the center undergo similar constraints and thermal expansions or contractions during cooling, producing nearly identical residual stress levels. This highlights the role of geometric symmetry and process uniformity in the simulation of residual stresses during quenching.

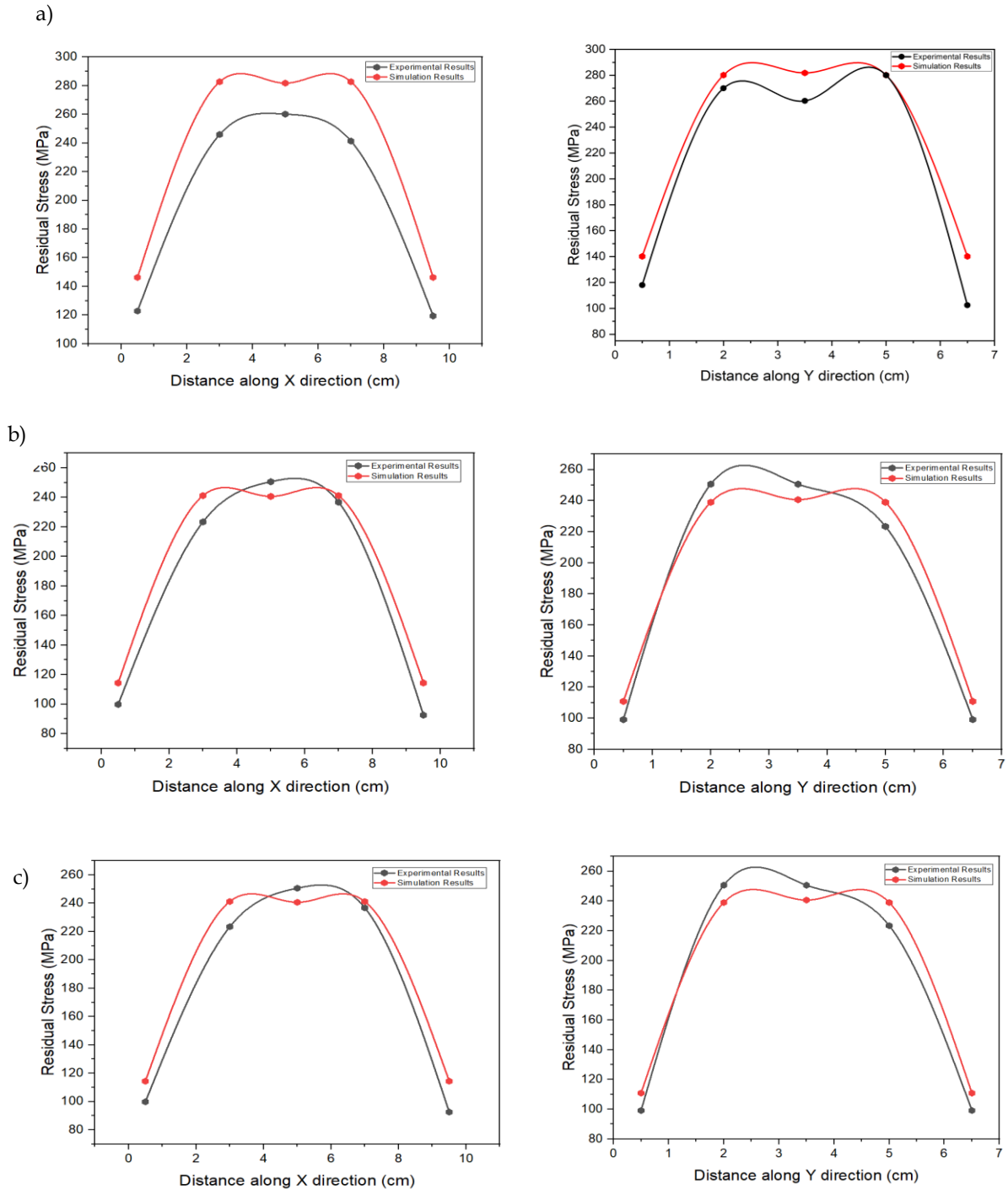


Figure 13. Comparison of experimental and simulation results for a) saltwater quenching b) water quenching and c) oil quenching

When residual stresses form, microstructural changes occur, such as the formation of dislocations or changes in grain structure, which can scatter and absorb ultrasonic waves, leading to increased attenuation. Also, applied external stress can result in microstructural changes in the material. These changes can include dislocation movement, grain reorientation, and the creation of defects. These microstructural changes can scatter and absorb ultrasonic waves, contributing to increased attenuation [16-20]. However, steel is a polycrystalline material, so ultrasonic attenuation is mainly caused by scattering the ultrasonic waves [14]. Considering Figure 6, which shows the variation in ultrasonic attenuation based on the quenching medium, it is observed that the maximum difference in attenuation coefficient occurs when salt water is used as the quenching medium, while the minimum difference is seen with oil as the medium.

It is crucial to understand that in the quenching process, residual stresses arising during a phase transformation are primarily due to the volume difference between the newly forming martensite phase and the initial austenite phase of the metallurgical structure. This phase transformation results in the expansion or contraction of the metal. When saltwater or water is used as the quenching medium, a more extensive transformation to martensite occurs due to their higher thermal conductivity. Therefore, Saltwater and water form larger martensite volume than austenite volume, exacerbating the development of internal stresses. Notably, saltwater, with its larger volume of martensite formation compared to water, leads to the maximum residual stress. Also, oil quenchants tend to produce a moderate grain structure with a more balanced composition of pearlite and martensite. This composition results in a smaller volume difference during phase transformation, and consequently, the magnitude of arising residual stresses is lower when compared to the other two quenching media.

Considering Figure 7, that figure shows that maximum residual stresses arise closer to the centre of the test specimen. When a steel test piece is quenched, the outer surface comes into direct contact with the quenching medium (e.g., water, oil, or saltwater) and cools rapidly. This rapid cooling creates a significant temperature gradient between the outer surface and the interior of the steel. As the outer surface of the steel cools and contracts more rapidly than the interior, it can induce tensile stresses on the surface. These stresses arise because the surface is trying to contract while the still-hot interior resists this contraction. In contrast, the interior of the steel remains relatively hot and undergoes less contraction. This can result in compressive stresses in the interior, where the material is attempting to expand but is constrained by the cooler outer layers. The combination of tensile stresses near the surface and compressive stresses in the interior can lead to a region of high-stress concentration near the center of the steel test piece [4, 21]. Besides that, phase transformations (transformation of austenite to martensite) can occur at different rates in the material, depending on the cooling rate. The center of the test piece, which cools more slowly, may undergo a different phase transformation process than the outer layers. This can lead to differential volume changes between the surface and center, further contributing to high residual stresses in the center plane [22].

The simulation results show that the maximum Von Mises residual stress occurs in the center plane of the specimen, with the stress gradually decreasing along the thickness direction. This can be explained by the previously discussed factors (thermal gradients and phase transformations). In addition to that, simulation results show maximum Von Mises residual stresses occur in the corners of the object compared with the center area. It happens because corners have a higher surface area-to-volume ratio compared to the center

of the piece. The corners are exposed to multiple cooling surfaces, including both the vertical and horizontal faces. As a result, they tend to cool more rapidly during quenching. The faster cooling rate can lead to a more significant temperature gradient and greater thermal gradients at the corners. The temperature gradients at the corners can be more severe than those in the central regions. These gradients result in non-uniform thermal expansion and contraction, leading to increased residual stresses [21].

However, experimental results (Figure 7) show some variations in residual stress at points equidistant from the center of the test piece, despite a symmetric setup and uniform quenching conditions. While symmetry and uniform quenching suggest that residual stresses should be consistent at symmetric points, real-world factors such as material inhomogeneity, quenching medium variability, and microstructural differences can lead to variations in these results [20, 23]. In the case of our material, AISI 1045, the non-uniform microstructure—such as variations in grain size (Figure 2), composition, or the presence of impurities—can cause differences in how the material responds to quenching, leading to disparities in residual stress. Even at symmetric points, slight variations in the microstructure across the test piece, influenced by factors like prior mechanical processing and heat treatment history, can affect the resulting stresses [23]. Additionally, the quenching medium may not cool the test piece uniformly due to issues like contamination and oxidation, and temperature gradients within the medium, further contributing to the differences in cooling rates at symmetric points, thereby causing variations in residual stress at some symmetric points [24].

There are always differences between simulation and experimental results. The experimental results are based on real-time system, which provides much more accurate results compared to simulation results. Obtaining the correct results from an experimental set-up is a challenge to any researcher. The difference is there due to the errors that occurred from external disturbances, instruments etc. Also, in this research thermal expansion coefficient and density were assumed to be temperature-independent in the simulation procedure. But in real situations, those two vary with temperature. Also, that affected the difference between simulation and experimental results. When we consider the experimental values, attenuation data is obtained through the thickness of this research. Considering from surface to center along the thickness direction, different planes have different residual stress values. The values are changed from compressive to tension from surface to center, and magnitudes are changed. So, different planes give different attenuation values along the thickness direction. Also, attenuation is increased under both compression and tensile stresses. So obtained attenuation difference gives an average magnitude value for residual stress [25, 26]. Therefore, we consider the center plane Von Mises stress values in ABAQUS to compare those experimental and simulation values. Since the center plane has maximum Von Mises residual stress and Von Mises stress always gives a positive value to residual stress.

## Conclusion

Considering the experimental and simulation results, it is evident that the attenuation method can effectively be used to determine the Von Mises residual stress values in the center plane of a quenched test specimen. The quenching process results in the maximum Von Mises residual stresses being concentrated in the center plane of the specimen. By accurately identifying these maximum stress values, we can infer critical information about the yield criteria of the material. This approach allows for a more precise

understanding of the material's stress distribution and its potential response to mechanical loading.

## References

- [1] Javadi, Y., Sadeghi, S., and Najafabadi, M.A., Taguchi optimization and ultrasonic measurement of residual stresses in the friction stir welding. *Materials & Design*, **2014**. 55, 27-34. 10.1016/j.matdes.2013.10.021.
- [2] Palanichamy, P., Vasudevan, M., and Jayakumar, T., Measurement of residual stresses in austenitic stainless steel weld joints using ultrasonic technique. *Science and Technology of Welding and Joining*, **2009**. 14(2), 166-171. 10.1179/136217108x394753.
- [3] Sharpe Jr, W.N. and Sharpe, W.N., *Springer handbook of experimental solid mechanics*. **2008**: Springer Science & Business Media.
- [4] Todinov, M.T., Mechanism for formation of the residual stresses from quenching. *Modelling and Simulation in Materials Science and Engineering*, **1998**. 6(3), 273-291. 10.1088/0965-0393/6/3/006.
- [5] Kočič, Š. and Figura, Z., Ultrasonic transducers, in *Ultrasonic Measurements and Technologies*, Š. Kočič and Z. Figura, Editors. **1996**, Springer US: Boston, MA. pp. 29-62.
- [6] John, Deepu & Karthik, Srinivas. (2014). Simulation of residual stress in quenched stainless steel spheres. 10.13140/RG.2.1.3263.4009.
- [7] Xiu, S., Deng, Y., and Kong, X., Effects of stress on phase transformations in grinding by FE modeling and experimental approaches. *Materials (Basel)*, **2019**. 12(14), 2327. 10.3390/ma12142327.
- [8] Fu, T., Chen, P., and Yin, A., A new axial stress measurement method for high-strength short bolts based on stress-dependent scattering effect and energy attenuation coefficient. *Sensors (Basel)*, **2022**. 22(13), 4692. 10.3390/s22134692.
- [9] Ploix, M.-A., Guy, P., Elguerjouma, R., Moysan, J., Corneloup, G., and Chassignole, B. Attenuation assessment for NDT of austenitic stainless steel welds. in *9th European Conference on NDT (ECNDT)*, Berlin. **2006**.
- [10] Kube, C.M. and Turner, J.A., Stress-dependent second-order grain statistics of polycrystals. *J. Acoust. Soc. Am.*, **2015**. 138(4), 2613-2625. 10.1121/1.4932026.
- [11] Ono, K., A comprehensive report on ultrasonic attenuation of engineering materials, including metals, ceramics, polymers, fiber-reinforced composites, wood, and rocks. *Appl. Sci. (Basel)*, **2020**. 10(7), 2230. 10.3390/app10072230.
- [12] Ohtani, T., Nishiyama, K., Yoshikawa, S., Ogi, H., and Hirao, M., Ultrasonic attenuation and microstructural evolution throughout tension-compression fatigue of a low-carbon steel. *Materials Science and Engineering: A*, **2006**. 442(1), 466-470. <https://doi.org/10.1016/j.msea.2006.02.226>.
- [13] Jurmey, K., Sharma Ghimire, N., Sivahar, V., Aravinda Abeygunawardane, G., and Piyathilake, M., *Prediction of true compressive flow stress of AA 6063 through ultrasonic attenuation*, in *2020 Moratuwa Engineering Research Conference (MERCOn)*. 2020, IEEE.
- [14] Aghaie-Khafri, M., Honarvar, F., and Zanganeh, S., Characterization of grain size and yield strength in AISI 301 stainless steel using ultrasonic attenuation measurements. *J. Nondestruct. Eval.*, **2012**. 31(3), 191-196. 10.1007/s10921-012-0134-z.
- [15] Samuel, A. and Prabhu, K.N., Residual stress and distortion during quench hardening of steels: A review. *J. Mater. Eng. Perform.*, **2022**. 31(7), 5161-5188. 10.1007/s11665-022-06667-x.

- [16] Kube, C.M. and Turner, J.A., Stress-dependent ultrasonic scattering in polycrystalline materials. *J. Acoust. Soc. Am.*, **2016**. 139(2), 811-824. 10.1121/1.4941253.
- [17] Chaudhary, S.K. and Sinha, V.K., Ultrasonic behavior of plastically deformed and heat treated steel. *Trans. Indian Inst. Met.*, **2008**. 61(2-3), 217-220. 10.1007/s12666-008-0033-2.
- [18] J. Krautkraemer, H. Krautkraemer, and W. Sachse, *Ultrasonic Testing of Materials*, vol. 51, no. 1. 1984. doi: 10.1115/1.3167589.
- [19] Arguelles, A.P. and Turner, J.A., Ultrasonic attenuation of polycrystalline materials with a distribution of grain sizes. *J. Acoust. Soc. Am.*, **2017**. 141(6), 4347. 10.1121/1.4984290.
- [20] E. P. Papadakis, "Ultrasonic Attenuation Caused by Scattering in Polycrystalline Media," in *Physical Acoustics*, 1968, pp. 269–328. doi: 10.1016/B978-0-12-395664-4.50018-3.
- [21] Nallathambi, A.K., Kaymak, Y., Specht, E., Bertram, A. (2008). Distortion and Residual Stresses during Metal Quenching Process. In: Bertram, A., Tomas, J. (eds) *Micro-Macro-interaction*. Springer, Berlin, Heidelberg. [https://doi.org/10.1007/978-3-540-85715-0\\_12](https://doi.org/10.1007/978-3-540-85715-0_12)
- [22] G. E. Totten, *Steel Heat Treatment*. CRC Press, 2006. doi: 10.1201/NOF0849384523.
- [23] Lu, S.-Q. and Chiu, L.-H., Effect of different microstructures on surface residual stress of induction-hardened bearing steel. *Metals (Basel)*, **2024**. 14(2), 201. 10.3390/met14020201.
- [24] D. S. MacKenzie, "Advances in quenching: A discussion of present and future technologies," *Gear Technology*, vol. 22, no. 2. pp. 20–26, 2005.
- [25] Finkel, P., Zhou, A.G., Basu, S., Yeheskel, O., and Barsoum, M.W., Direct observation of nonlinear acoustoelastic hysteresis in kinking nonlinear elastic solids. *Appl. Phys. Lett.*, **2009**. 94(24), 241904. 10.1063/1.3155201.
- [26] G. Gremaud, S. L. Kustov, and O. Bremnes, "9.2 Ultrasonics Techniques: PUCOT and ACT," *Mater. Sci. Forum*, vol. 366–368, no. January 2001, pp. 652–666, Mar. 2001, doi: 10.4028/www.scientific.net/MSF.366-368.652.